Published in final edited form as:
Brain Res. 2005 May 10; 1043(1-2): 155–162. doi:10.1016/j.brainres.2005.02.073.

Perfusion and diffusion imaging in acute focal cerebral ischemia: Temporal vs. spatial resolution

Juergen Bardutzky[a,e,*], **Qiang Shen**[b], **James Bouley**[a], **Christopher H. Sotak**[c,d], **Timothy Q. Duong**[a,b], and **Marc Fisher**[a,c]

[a]Department of Neurology, University of Massachusetts Medical School, Boston, MA 02125, USA

[b]Center for Comparative NeuroImaging, Department of Psychiatry, University of Massachusetts Medical School, Boston, MA 02125, USA

[c]Department of Radiology, University of Massachusetts Medical School, Boston, MA 02125, USA

[d]Department of Biomedical Engeneering, Worcester Polytechnic Institute, Worcester, MA 01609, USA

[e]Department of Neurology, University of Heidelberg, Germany

Abstract

High-resolution diffusion- (DWI) and perfusion-weighted (PWI) imaging may provide substantial benefits in accurate delineation of normal, ischemic, and at-risk tissue. We compared the capability of low (400 × 400 μm^2) and high (200 × 200 μm^2) spatial resolution imaging in characterizing the spatiotemporal evolution of the ischemic lesion in a permanent middle artery occlusion (MCAO) model in rats. Serial measurements of cerebral blood flow (CBF) and the apparent diffusion coefficient (ADC) were performed. Lesion volumes were calculated by using viability thresholds or by visual inspection, and correlated with infarct volume defined by TTC staining at 24 h after MCAO. At the very early phase of ischemia, high-resolution resulted in a significantly larger ADC-derived lesion volume and a smaller PWI/DWI mismatch. At 3 h after MCAO, ADC and CBF lesions showed similar robust correlations with TTC-defined infarct volumes for both groups using previously established thresholds. When lesions were determined visually, low-resolution resulted in a substantial overestimation of TTC-defined infarct volume and a lower inter-observer reliability (r = 0.75), whereas high-resolution produced an excellent correlation with TTC-defined infarct volume and inter-observer reliability (r = 0.96). In conclusion, high-resolution MRI resulted in substantial temporal averaging of the ischemic lesion during the early phase, but was clearly superior in visual determination of final infarct size. Low-resolution reasonably evaluated the temporal and spatial evolution of ischemia when thresholds were used.

Keywords

Focal ischemia; Perfusion–diffusion mismatch; High-resolution imaging; ADC; CBF

[*]Corresponding author. Department of Neurology, University of Heidelberg, INF 400, 69120 Heidelberg, Germany. Fax: +49 6221 564671. juergen.bardutzky@med.uni-heidelberg.de (J. Bardutzky).

1. Introduction

Diffusion-weighted (DWI) and perfusion-weighted (PWI) magnetic resonance imaging (MRI) are powerful imaging modalities for the early detection of ischemic brain injury in both experimental [3] and human stroke [9]. The region with perfusion abnormality but without diffusion abnormality, commonly referred to as “diffusion/perfusion mismatch”, is thought to represent an approximation of the ischemic penumbra [16].

The spatiotemporal evolution of the ischemic lesion during the acute phase of cerebral ischemia is a highly dynamic process, as the diffusion/perfusion mismatch gradually decreases over time [7], and thus represents a rapidly moving target. In order to accurately assess pathophysiological dynamics, good temporal resolution, using short image acquisition times, is necessary. However, the need for good temporal resolution in the acute stroke setting limits spatial resolution, resulting in relatively poor spatial discrimination, and may produce misclassification of pixels based on bioenergetic and hemodynamic characteristics, especially in the mismatch region. Minimizing partial volume by improving spatial resolution yields better discrimination of tissue boundaries, resulting in a more precise identification of normal, ischemic core, and “at-risk-to-infarction” tissue. A clear visual delineation may be of particular importance in human MRI studies where lesion volumes are usually determined by manually tracing the lesion border [4,13,14], rather than applying viability thresholds, and could reduce observer bias in the interpretation of human stroke MRI.

High-resolution MRI, on the other hand, requires longer acquisition time and may result in temporal averaging of the ischemic evolution, resulting in an inadequate reflection of the actual ischemic progression. Thus, acute stroke MRI is a compromise between appropriate temporal and spatial resolution. In experimental stroke, most investigators use a relatively low in-plane resolution of approximately 400 × 400 μm^2, with a PWI/DWI acquisition time of a few minutes [3,6,8,10,11,17,21,22]. It remains unclear whether high-resolution imaging provides substantial benefits in accurate classification of tissue fate and whether the improvements in spatial discrimination justify the poor temporal resolution in the acute phase of ischemia. In the present study, the main goal was to compare the ability of high spatial resolution (200 × 200 μm^2) and the commonly used low-resolution (400 × 400 μm^2) imaging in characterizing the spatial and temporal evolution of ischemia in a permanent occlusion model in rats.

2. Methods

2.1. Animal preparations

Male Sprague–Dawley rats (n = 14, 300–350 g, Taconic Farms, NY, USA) were initially anesthetized with chloral hydrate (400 mg/kg ip). Rectal temperature was kept at 37 ± 0.5°C throughout the entire experiment using a feedback-controlled heating pad. PE-50 tubing was inserted into the right femoral artery for continuous monitoring of arterial blood pressure and heart rate, and for blood-gas sampling immediately before and 3.5 h after induction of ischemia.

Permanent focal cerebral ischemia was produced by intraluminal suture occlusion of the right middle cerebral artery (MCAO), as previously described [6]. Immediately after occlusion, the animals were positioned in a stereotaxic headholder and quickly placed into the magnet. Once the animal was in the magnet, anesthesia was switched to 1.25% isoflurane delivered in air at 1.5 L/min.

Twenty-four hours after MCAO, the brains were cut into eight 1.5-mm-thick coronal slices corresponding to the MRI slices and stained with 2,3,5-triphenyltatrazolium chloride (TTC). To compensate for the effects of brain edema, corrected infarct volume was calculated as previously described [7].

2.2. MR imaging measurements

Magnetic resonance imaging was performed on a Bruker 4.7 T/40 cm horizontal magnet (Billerica, MA) and a 20 G/cm magnetic field gradient insert. For optimal comparison of the different spatial resolutions, identical MRI parameters were used except for the matrix size. All images were acquired with a 2.56 × 2.56 cm^2 field of view and eight 1.5 mm slices.

The average apparent diffusion coefficient (ADC_{av}) of water was obtained by averaging three ADC maps acquired separately with diffusion-sensitive gradients applied along the *x*, *y*, or *z* direction. High-resolution data were acquired using four-segment, spin-echo, echo-planar images (EPI) with a 128 × 128 matrix; other parameters were spectral width = 200 kHz, TR = 2 s (90° flip angle), b = 10 and 1269 s/mm^2, TE = 37.5 ms, Δ = 17.53 ms, δ = 5.6 ms, diffusion gradient amplitude (*G*) = 10 and 190 mT/m, and 16 averages (total acquisition time = 8:53 min). Low-resolution data were acquired using identical parameters, except single-shot EPI and a 64 × 64 matrix (total acquisition time = 2:13 min).

Quantitative cerebral blood flow (CBF) measurements were carried out using the continuous arterial spin-labeling (ASL) technique, as previously described in details [17]. Briefly, paired images were acquired alternately, one with arterial spin-labeling and the other without spin-labeling preparation (control). High-resolution data were acquired using four-segment, gradient-echo EPI with a 128 × 128 matrix, TR = 2 s, TE = 14.4 ms. 76 pairs of ASL scans were acquired in two separate sets of 38 pairs each, one set obtained before, and the other after the ADC measurements (total acquisition time = 20 min). Low-resolution data were acquired using identical parameters, except single-shot GE EPI with a 64 × 64 matrix (total acquisition time = 4:93 min).

2.3. Experimental protocol

This study consisted of two different groups: (1) low-resolution group (L-R, *n* = 7), and (2) high-resolution group (H-R, *n* = 7). The total acquisition time for a complete ADC_{av} and CBF data set was ~30 min for high-resolution and ~7.5 min for low-resolution. The post-occlusion time quoted was at the middle of the MRI acquisition at each time point. The first imaging block was started 20 min after MCAO in both groups. In the H-R group, imaging was performed continuously with an ADC/CBF data set acquired 35, 65, 95,125, and 180 min after MCAO. The timetable for the L-R group was chosen in order to achieve the following aims: (1) to compare temporal resolution during the very early phase of ischemia (i.e., up to 80 min post-occlusion), each of the first two high-resolution data sets was covered by two low-resolution blocks (24 and 46 min, and 54 and 76 min after MCAO); (2) to compare high and low-resolution at same time points, the middle of a low-resolution data set matched the middle of a high-resolution scan at 95, 125, and 180 min; (3) the 180-min data set in each group was followed by an additional data set of the opposite resolution at 200 min to compare the two sets in the same animal. ADC- and CBF-defined lesions should not differ much at these time points because ischemia stops evolving after 3 h in this permanent occlusion model [7,17,12].

2.4. Data analysis

MRI measurements were analyzed using the imaging processing programs Matlab (math-Works, Natick, MA, USA) and STIMULATE software [20]. Quantitative ADC_{av} maps, in units of square millimeters per second, were calculated using the Stejskal–Tanner equation [19]. CBF maps, in units of milliliters per gram of tissue per minute, were calculated using the water–blood partition coefficient λ of 0.9, tissue T1 of 1.5 s, and spin-labeling efficiency α of 0.75 [1,18].

2.4.1. Calculation of in vitro lesion size

2.4.1.1. Based on viability thresholds—In the same permanent ischemia model, ADC and CBF viability thresholds have been previously determined by setting the ADC- and CBF-derived lesion volumes at 3 h equal to the infarct volume defined by TTC at 24 h post-occlusion [7,17]. The 3-h time point was chosen because DWI-defined lesion volume was shown to stop growing by 150–180 min after permanent MCAO and highly correlates with the infarct volume determined by postmortem histology [12]. These thresholds, 0.53×10^{-3} mm^2/s for ADC and 0.30 ml/g/min for CBF, were used to identify all pixels with abnormal ADC or CBF characteristics on each of the eight imaged slices at each time point. The ADC- and CBF-derived lesion volumes at 180 and 200 min (opposite resolution to 180 min in the same animal) were correlated with TTC-derived infarct volumes at 24 h.

2.4.1.2. Based on visual determination—Abnormal ADC and CBF volumes were determined visually by an investigator blinded to imaging groups (JB). The edge of the lesions at 180 and 200 min post-occlusion was traced manually on each of the eight coronal slices for each animal. The areas of hypointensity were then summed and multiplied by slice thickness. Visually defined lesion volumes were correlated with the TTC-derived infarct volumes. Data were also analyzed by a second observer (JBo) to determine the inter-observer reliability.

2.5. Statistical analysis

Data are presented as mean ± standard deviation. Statistical analysis was performed with repeated-measures ANOVA when testing for differences among different time points in individual groups. A two-tail unpaired *t* test was used to compare the parametric values. Linear regression analysis was performed to correlate the ADC- and CBF-derived lesion volumes with TTC-defined infarct volumes and to compare lesion volumes between observers. A two-tail *P* value of <0.05 was considered to be significant.

3. Results

Blood gases (pO_2, pCO_2, pH), heart rate, mean arterial blood pressure, and rectal temperature were within normal range throughout and were not statistically different between groups or across different time points (data not shown).

3.1. Quantitative ADC and CBF values

In the nonischemic left hemisphere (LH), CBF and ADC values were stable across all time points and were not statistically different between groups. The average CBF and ADC values were 1.18 ± 0.18 ml/g/min and $0.75 \pm 0.03 \times 10^{-3}$ mm^2/s for the H-R group and 1.23 ± 0.25 ml/g/min and $0.75 \pm 0.02 \times 10^{-3}$ mm^2/s for the L-R group.

In the ischemic right hemisphere (RH), CBF was constantly lower at all time points for both groups compared to the normal LH (H-R: 35 ± 2% of LH; L-R: 37 ± 2% of LH; $P < 0.0001$ each). ADC values in the RH gradually decreased over time in both groups. When comparing the first data set (starting at 20 min post-occlusion), mean ADC values were significantly lower in the H-R group ($0.61 \pm 0.02 \times 10^{-3}$ mm^2/s) compared to those in the L-R group ($0.65 \pm 0.02 \times 10^{-3}$ mm^2/s; $P < 0.05$), suggesting a further decrease in ADC during the 30-min acquisition time required for high-resolution imaging. The difference was not significant between the data sets starting at 50 min (0.58 ± 0.02 vs. 0.60 ± 0.03; $P = 0.14$) and disappeared entirely at later time points.

3.2. Temporal evolution of lesion volumes using viability thresholds

Fig. 1 shows the temporal evolution of ADC and CBF lesion volumes using previously established thresholds. As expected in a permanent occlusion model, CBF-derived lesion volume remained relatively constant across all time points in both groups ($P > 0.05$). The TTC-defined infarct volumes 24 h after occlusion were slightly smaller than the CBF-derived lesion volumes at 180 min for both H-R (270 ± 50 vs. 276 ± 42 mm^3) and L-R (259 ± 55 vs. 269 ± 37 mm^3) group. To minimize inter-group differences, the 180-min data set was followed by an additional data set of the opposite resolution at 200 min post-occlusion in each animal for both groups. There were similar high correlation and correspondence between CBF-derived lesion volumes at 180/200 min and TTC-defined infarct volumes for both high-resolution (correlation coefficient $r = 0.94$, one-to-one-correspondence ($y = x$) coefficient $R = 1.02$, $P < 0.001$) and low-resolution ($r = 0.94$, $R = 1.04$, $P < 0.001$).

The temporal evolution of the ADC-derived lesion volumes differed significantly between the two groups during the very early phase of ischemia. At the first time point obtained after MCAO, ADC-defined lesion volume was significantly larger in the H-R group (178 ± 34 mm^3) as compared to that in the L-R group (125 ± 40 mm^3, $P < 0.05$). This difference was still present when comparing the data sets starting 50 min after occlusion, but was not significant ($P = 0.14$). There was no difference in ADC lesion volume between groups at later time points, and at 180 min after MCAO the ADC-derived lesion volumes were essentially identical to the TTC infarct volumes in both groups. When analyzing the ADC-derived lesion volume at 180 and 200 min (opposite resolution in the same animal), the lesion size did not differ significantly and showed an excellent correlation and correspondence with the TTC-defined infarct volume at 24 h for both high-resolution ($r = 0.97$, $R = 0.96$, $P < 0.001$) and low-resolution ($r = 0.98$, $R = 0.98$, $P < 0.001$).

In the L-R group, the diffusion/perfusion mismatch identified as the difference between abnormal diffusion and perfusion volume was significant at 24, 46, and 56 min after MCAO (57%, 34%, and 30% of abnormal perfusion volume, $P < 0.01$ each), whereas in the H-R group, the diffusion/perfusion mismatch was only significant at 35 min (35% of abnormal perfusion volume, $P < 0.001$). By 3 h after occlusion, the abnormal diffusion volume was 97% and 96% of the abnormal perfusion volume in the H-R and L-R group, respectively.

3.3. Visual estimation of lesion volumes at 180 and 210 min

Fig. 2 shows representative ADC and CBF maps at 180 and 200 min from one animal. High-resolution produced an excellent correlation and one-to-one correspondence between the visually-defined abnormal MRI volume at 180/200 min and the TTC-derived infarct volume at 24 h (ADC: $r = 0.98$, $R = 0.98$; CBF: $r = 0.98$, $R = 1.05$; $P < 0.0001$ each; Figs. 3a and b). The average visually delineated abnormal CBF volume (278 ± 46 mm^3) was slightly larger than TTC-defined infarct volume (264 ± 50 mm^3), whereas the visually delineated ADC lesion volume (260 ± 47 mm^3) was essentially identical to TTC infarct volume. In contrast, using low-resolution, the visually defined MRI lesion volumes at 180/200 min differed significantly compared to the TTC-defined infarct volume, with the mean lesion volume being 313 ± 57 mm^3 ($P < 0.05$) for diffusion and 328 ± 53 mm^3 ($P < 0.01$) for perfusion imaging. The slope (R) of the regression line of 1.18 for ADC and 1.23 for CBF lesion volumes clearly indicated a substantial overestimation in visually MRI-defined lesion volumes when compared with TTC-defined infarct volume at 24 h (Figs. 3a and b). This overestimation of lesion volume by visual determination was consistently observed in each of the 14 animals in both ADC and CBF images and it was more pronounced in perfusion-weighted imaging.

To investigate the inter-observer reliability, all data sets at 180 and 200 min after MCAO were analyzed by a second investigator blinded to the previous results (JBo). Fig. 4 shows the

correlation of visually identified ADC (a) and CBF (b) lesion volumes between the two observers. The overall inter-observer reliability was markedly lower when using low-resolution ($r = 0.75$ vs. $r = 0.96$ for high-resolution) and was more pronounced for CBF imaging ($r = 0.67$ vs. $r = 0.95$). Mean ADC and CBF lesion volumes identified with high-resolution were not significantly different between the observers (ADC: 260 ± 47 vs. 275 ± 59 mm^3; CBF: 278 ± 46 vs. 292 ± 53 mm^3). In contrast, using low-resolution, the results between the two observers differed significantly for both ADC (313 ± 57 vs. 367 ± 68 mm^3, $P < 0.05$) and CBF lesion volumes (328 ± 53 vs. 380 ± 65 mm^3, $P < 0.05$).

4. Discussion

The major findings in the present study were (1) high-resolution imaging resulted in substantial temporal averaging of the ischemic lesion at early time points post-occlusion; (2) when using viability thresholds, low-resolution imaging accurately predicted the final TTC-defined infarct volume and was comparable to high-resolution; (3) when abnormal diffusion and perfusion volumes were evaluated by visual inspection, high-resolution imaging yielded improved accuracy and inter-observer reliability, whereas low-resolution persistently overestimated lesion size and had a poorer inter-observer reliability.

The major drawback of high-resolution imaging is the long acquisition time. The acquisition time used in the present study was 30 min, four times longer compared to low-resolution (four-segment vs. single-shot EPI). The long acquisition time resulted in a markedly reduced capability to detect different stages of ischemic lesion evolution during the early phases. As demonstrated by the low-resolution data, the ADC-derived lesion volume increased rapidly and significantly during the 30-min period of high-resolution acquisition, especially during the first 60 min following occlusion. As a consequence of the long acquisition time and temporal averaging of early phase ischemia progression, the identification of the diffusion/perfusion mismatch, the main target of stroke therapy [16], differed significantly between high and low-resolution imaging. The temporal progression of ischemia, however, represents an important end point in studying the in vivo effects and efficacy of novel therapeutic approaches in experimental stroke. Thus, high-resolution is not recommended for MRI studies focusing on the temporal evolution of ischemia during the very early phase in this stroke model.

Ischemia-induced partial volume effects could be more severe at the boundaries between normal and abnormal brain tissue. The stroke model used in the present study produced a large infarction of the entire MCA territory, resulting in a relatively small surface-to-volume ratio. Ischemia-induced partial volume effects may be more evident in small infarcts with larger surface-to-volume ratio such as in lacunar stroke.

Using viability thresholds, the standard deviations for lesion volumes were similar for high and low-resolution imaging, suggesting that the main source of variance is inter-animal differences. This inter-animal variance may obscure differences between high and low-resolution imaging.

Another drawback of high-resolution imaging is a reduced signal-to-noise ratio (SNR). Although the number of signal averages at high-resolution was kept the same as low-resolution, semi-quantitative comparison showed that SNR at high-resolution was 2–3 times lower than that at low-resolution, instead of the expected factor of 4 (data not shown). Quantitative analysis of SNR was difficult because a small FOV was used and thus a “noise” region free of ghosting was difficult to identify. The reduced intravoxel dephasing and its effect on signal decays at high-resolution could partially compensate the SNR loss.

Using the previously validated thresholds, low-resolution imaging provided an accurate assessment of final lesion size in this stroke model and was comparable to high-resolution. In

experimental stroke, the ischemic lesion is usually determined by using viability thresholds rather than visual inspection [2,3,7,10,17]. Our findings showed that high-resolution imaging did not offer notable advantages over low-resolution imaging in determining the final spatial extent of ischemic lesion when viability thresholds were used. The good correlation between threshold-derived MRI lesion volumes on low-resolution imaging and TTC lesion volumes was expected as the thresholds used were defined by their agreement with the 24-h TTC lesion in a previous study in the same model [7]. Re-evaluating the viability thresholds for high-resolution revealed essentially identical thresholds (data not shown), suggesting that the viability thresholds were essentially independent on the spatial resolution in this stroke model.

Visual determination of ischemic lesion volumes yielded markedly different results between high- and low-resolution imaging. Increasing the number of pixels by a factor of four produced a clearer visual delineation of the boundary between abnormal and normal tissue. Consequently, high-resolution lesion volumes showed an excellent correlation and correspondence with the histologically defined infarct volume and between different observers. In contrast, low-resolution resulted in an inadequate assessment of final lesion volume, with a substantial overestimation of eventual infarct size. This effect was found in both the diffusion and perfusion imaging data sets, but was more pronounced for perfusion-weighted imaging, possibly due to a lower SNR and/or large dynamic ranges. Furthermore, the inter-observer reliability was reduced with low-resolution imaging, reflecting the individual variability in proper identification of abnormal and normal tissue due to relatively imprecise boundaries. Thus, when using visual determination, high-resolution is recommended for more accurate delineation of final lesion size when ischemic lesion is stable and temporal resolution is less of a factor.

The reason for persistent overestimation of visually defined lesion size in low-resolution imaging is unclear. The ADC or CBF of a single low-resolution pixel could be approximated by a weighted average of the four high-resolution pixels. Herein, in the border of normal-abnormal area, the ADC or CBF of a single low-resolution pixel was heavily weighted by the low “ischemic” core ADC or CBF. This may result in a moderately reduced (but above the threshold) ADC or CBF of a single low-resolution pixel. However, the differences in gray intensity were minimal between tissues with severely and moderately reduced ADC or CBF values and it was difficult to distinguish pixels within this small range by visual inspection. Thus, it is likely that pixels with moderately reduced values were included in the visually defined lesion area resulting in a persistent overestimation of the actual lesion size. Another explanation may be the fact that the area with severely reduced CBF destined to infarction is typically surrounded by a small outer rim of tissue experiencing benigne oligemia (above the viability threshold) [5]. Possibly, this area of benigne oligemia was included in the visually defined CBF lesion area as the separation of this tissue from tissue with severely reduced CBF was difficult by simple visual inspection. This may also explain the finding that even high-resolution imaging resulted in a slight but persistent overestimation of visually defined CBF lesion volume, as illustrated in Fig. 3b.

Although differences in the spatiotemporal evolution of stroke lesion between animal models and humans have been reported [6,15], the observations in our study may be of potential clinical relevance. In human stroke studies, abnormal diffusion and perfusion regions are identified by visual inspection and outlined manually [4,13,14]. Physicians should be aware that a lower spatial resolution may be associated with a substantial overestimation of final infarct size and an increased risk of observer bias in interpretation of stroke MRI, whereas high-resolution produced high accuracy and inter-observer reliability. The long acquisition time for high-resolution, however, resulted in a substantial temporal averaging of lesion volume evolution in the very early phase of experimental ischemia. The issue of temporal averaging is likely to be less evident in human stroke since by the time most patients get MRI the progression of

ischemic lesion during a 30-min interval is expected to be small. Still, the use of high-resolution imaging in acute stroke patients is severely constrained by limited imaging time. Further increases in spatial and/or temporal resolution are expected with improvement in MRI technologies, offering the potential for routine high spatiotemporal imaging of acute stroke.

5. Conclusion

Our results demonstrated that both high and low-resolution imaging have advantages as well as disadvantages in evaluating the acute phase of ischemia, and the use of one over the other depends largely on a study's underlying focus. High-resolution imaging resulted in a substantial temporal averaging of the ischemic lesion during the early phase, but was clearly superior in visual determination of final infarct size. Using viability thresholds, low-resolution imaging was capable of reasonably evaluating the temporal and spatial evolution of ischemia.

References

1. Duong TQ, Silva AC, Lee SP, Kim SG. Functional MRI of calcium-dependent synaptic activity: cross correlation with CBF and BOLD measurements. Magn. Reson. Med 2000;43:383–392. [PubMed: 10725881]
2. Ebisu T, Mori Y, Katsuta K, Fujikawa A, Matsuoka N, Aoki I, Umeda M, Naruse S, Tanaka C. Neuroprotective effects of an immunosuppressant agent on diffusion/perfusion mismatch in transient focal ischemia. Magn. Reson. Med 2004;51:1173–1180. [PubMed: 15170837]
3. Hoehn-Berlage M, Norris DG, Kohno K, Mies G, Leibfritz D, Hossmann KA. Evolution of regional changes in apparent diffusion coefficient during focal ischemia of rat brain: the relationship of quantitative diffusion NMR imaging to reduction in cerebral blood flow and metabolic disturbances. J. Cereb. Blood Flow Metab 1995;15:1002–1011. [PubMed: 7593332]
4. Kidwell CS, Saver JL, Mattiello J, Starkman S, Vinuela F, Duckwiler G, Gobin YP, Jahan R, Vespa P, Villablanca JP, Liebeskind DS, Woods RP, Alger JR. Diffusion–perfusion MRI characterization of post-recanalization hyperperfusion in humans. Neurology 2001;57:2015–2021. [PubMed: 11739819]
5. Kidwell CS, Alger JR, Saver JL. Beyond mismatch: evolving paradigms in imaging the ischemic penumbra with multimodal magnetic resonance imaging. Stroke 2003;34:2729–2735. [PubMed: 14576370]
6. Li F, Silva MD, Sotak CH, Fisher M. Temporal evolution of ischemic injury evaluated with diffusion-, perfusion-, and T2-weighted MRI. Neurology 2000;54:689–696. [PubMed: 10680805]
7. Meng X, Fisher M, Shen Q, Sotak CH, Duong TQ. Characterizing the diffusion/perfusion mismatch in experimental focal cerebral ischemia. Ann. Neurol 2004;55:207–212. [PubMed: 14755724]
8. Nagel S, Wagner S, Koziol J, Kluge B, Heiland S. Volumetric evaluation of the ischemic lesion size with serial MRI in a transient MCAO model of the rat: comparison of DWI and T1WI. Brain Res. Brain Res. Protoc 2004;12:172–179. [PubMed: 15013468]
9. Neumann-Haefelin T, Moseley ME, Albers GW. New magnetic resonance imaging methods for cerebrovascular disease: emerging clinical applications. Ann. Neurol 2000;47:559–570. [PubMed: 10805325]
10. Olah L, Wecker S, Hoehn M. Relation of apparent diffusion coefficient changes and metabolic disturbances after 1 hour of focal cerebral ischemia and at different reperfusion phases in rats. J. Cereb. Blood Flow Metab 2001;21:430–439. [PubMed: 11323529]
11. Petty MA, Neumann-Haefelin C, Kalisch J, Sarhan S, Wettstein JG, Juretschke HP. In vivo neuroprotective effects of ACEA 1021 confirmed by magnetic resonance imaging in ischemic stroke. Eur. J. Pharmacol 2003;474:53–62. [PubMed: 12909195]
12. Reith W, Hasegawa Y, Latour LL, Dardzinski BJ, Sotak CH, Fisher M. Multislice diffusion mapping for 3-D evolution of cerebral ischemia in a rat stroke model. Neurology 1995;45:172–177. [PubMed: 7824111]
13. Rother J, Schellinger PD, Gass A, Siebler M, Villringer A, Fiebach JB, Fiehler J, Jansen O, Kucinski T, Schoder V, Szabo K, Junge-Hulsing GJ, Hennerici M, Zeumer H, Sartor K, Weiller C, Hacke W. Kompetenznetzwerk Schlaganfall Study Group. Effect of intravenous thrombolysis on MRI

parameters and functional outcome in acute stroke <6 hours. Stroke 2002;33:2438–2445. [PubMed: 12364735]

14. Schellinger PD, Fiebach JB, Jansen O, Ringleb PA, Mohr A, Steiner T, Heiland S, Schwab S, Pohlers O, Ryssel H, Orakcioglu B, Sartor K, Hacke W. Stroke magnetic resonance imaging within 6 hours after onset of hyperacute cerebral ischemia. Ann. Neurol 2001;49:460–469. [PubMed: 11310623]
15. Schlaug G, Siewert B, Benfield A, Edelman RR, Warach S. Time course of the apparent diffusion coefficient (ADC) abnormality in human stroke. Neurology 1997;49:113–119. [PubMed: 9222178]
16. Schlaug G, Benfield A, Baird AE, Siewert B, Lovblad KO, Parker RA, Edelman RR, Warach S. The ischemic penumbra: operationally defined by diffusion and perfusion MRI. Neurology 1999;53:1528–1537. [PubMed: 10534263]
17. Shen Q, Meng X, Fisher M, Sotak CH, Duong TQ. Pixel-by-pixel spatiotemporal progression of focal ischemia derived using quantitative perfusion and diffusion imaging. J. Cereb. Blood Flow Metab 2003;23:1479–1488. [PubMed: 14663344]
18. Silva AC, Lee SP, Yang G, Iadecola C, Kim SG. Simultaneous blood oxygenation level-dependent and cerebral blood flow functional magnetic resonance imaging during forepaw stimulation in the rat. J. Cereb. Blood Flow Metab 1999;19:871–879. [PubMed: 10458594]
19. Stejkal EO, Tanner JE. Spin diffusion measurements: spin echoes in the presence of a time-dependent field gradient. J. Chem. Phys 1965;42:288–292.
20. Strupp JP. Stimulate: a GUI based fMRI analysis software package. NeuroImage 1996;3:S607.
21. van Lookeren Campagne M, Thomas GR, Thibodeaux H, Palmer JT, Williams SP, Lowe DG, van Bruggen N. Secondary reduction in the apparent diffusion coefficient of water, increase in cerebral blood flow volume, and delayed neuronal death after middle cerebral artery occlusion and reperfusion in the rat. J. Cereb. Blood Flow Metab 1999;19:1354–1364. [PubMed: 10598940]
22. Wang L, Yushmanov VE, Liachenko SM, Tang P, Hamilton RL, Xu Y. Late reversal of cerebral perfusion and water diffusion after transient focal ischemia in rats. J. Cereb. Blood Flow Metab 2002;22:253–261. [PubMed: 11891430]

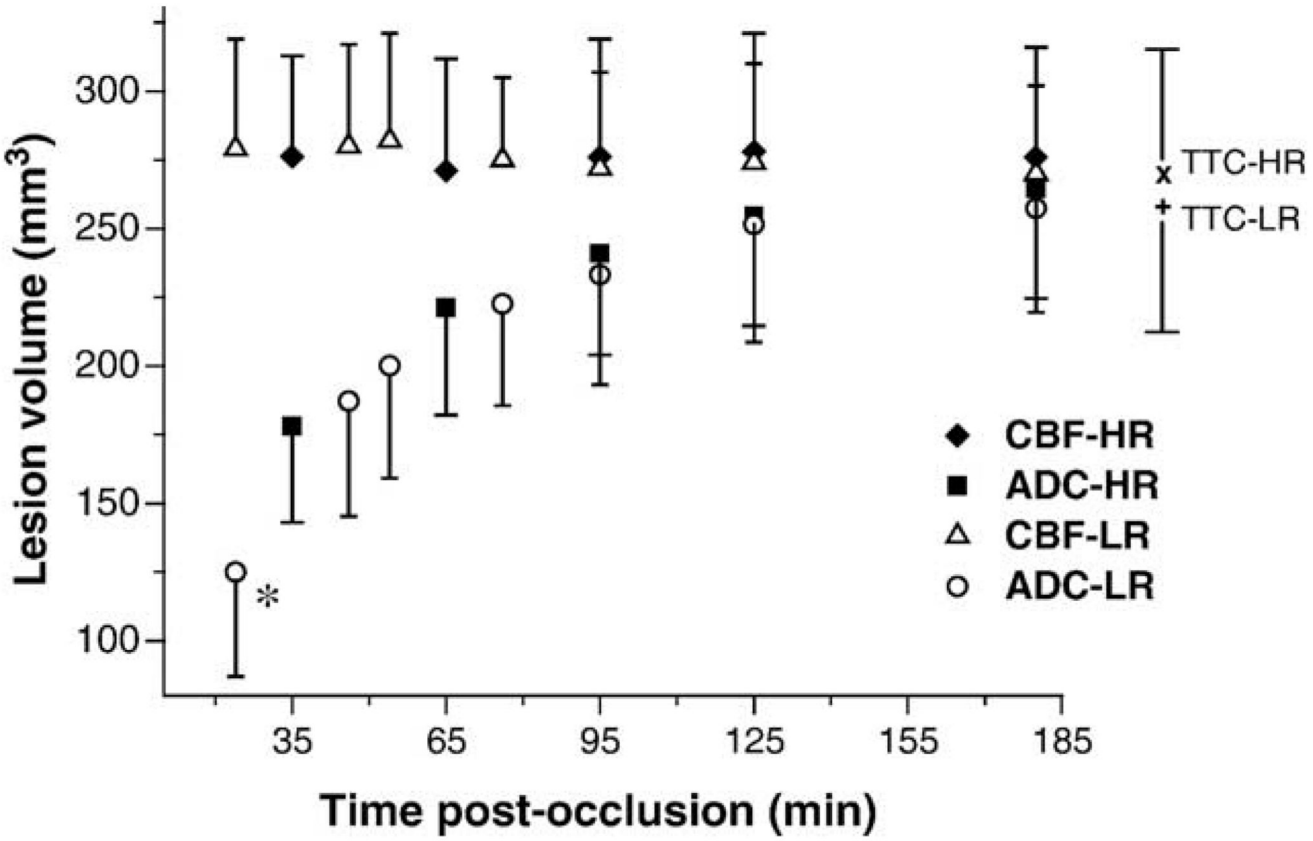

Fig. 1.

Temporal evolution of MRI-derived lesion volumes (mean ± SD) by using viability thresholds. CBF lesion: closed diamonds = high-resolution; open triangles = low-resolution. ADC lesion: closed squares = high-resolution; open circles = low-resolution. x = TTC lesion at 24 h after MCAO for high-resolution group; + = TTC lesion at 24 h after MCAO for low-resolution group. *$P < 0.05$ vs. ADC lesion at 35 min (high-resolution).

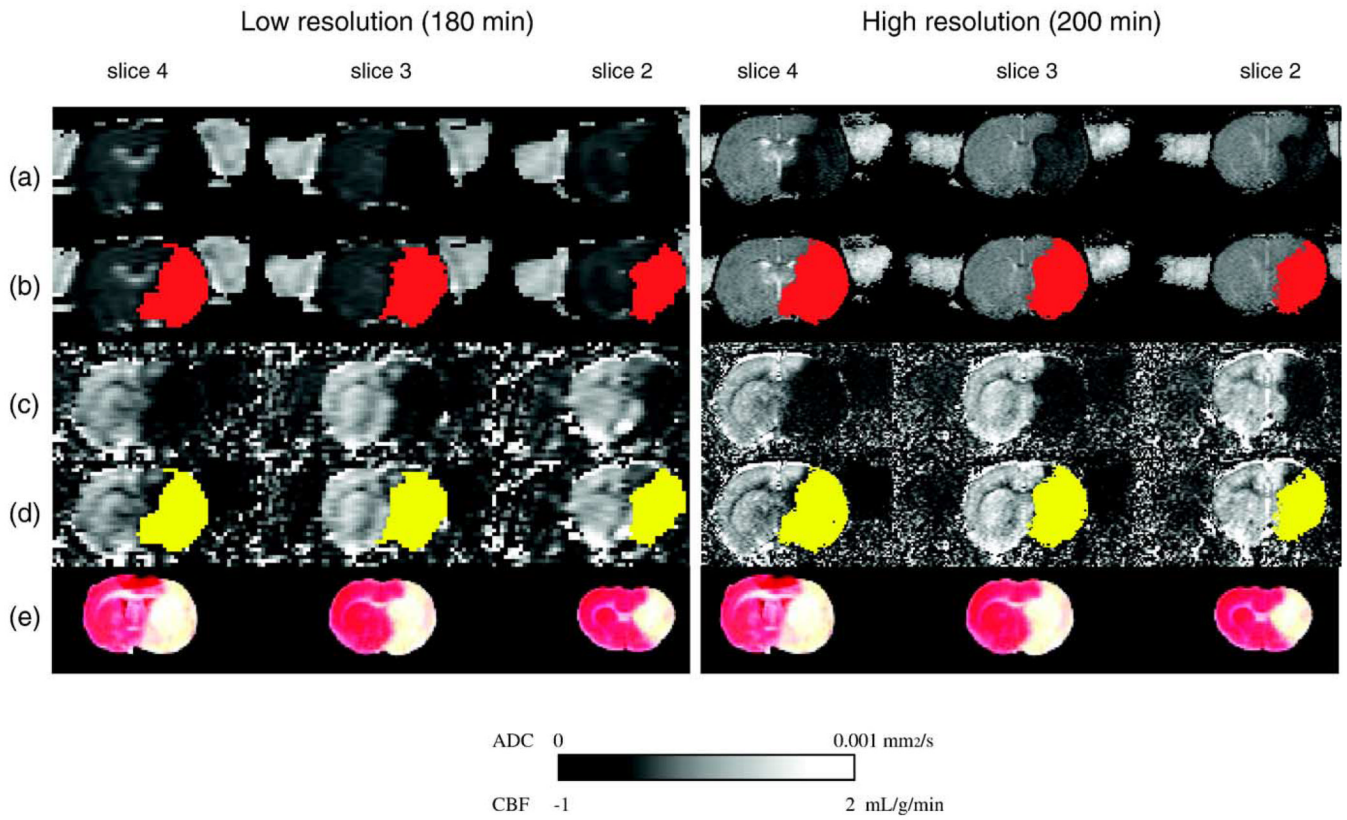

Fig. 2.

Representative ADC (a) and CBF (c) maps from one animal (group L-R). Three of eight multislice maps are shown at 180 (low-resolution) and 200 min (high-resolution) after MCAO. The ADC-derived (b, red) and CBF-derived (d, yellow) lesion volumes determined by high- and low-resolution are almost identical when using viability thresholds and matched well with the TTC-defined infarct volume (e).

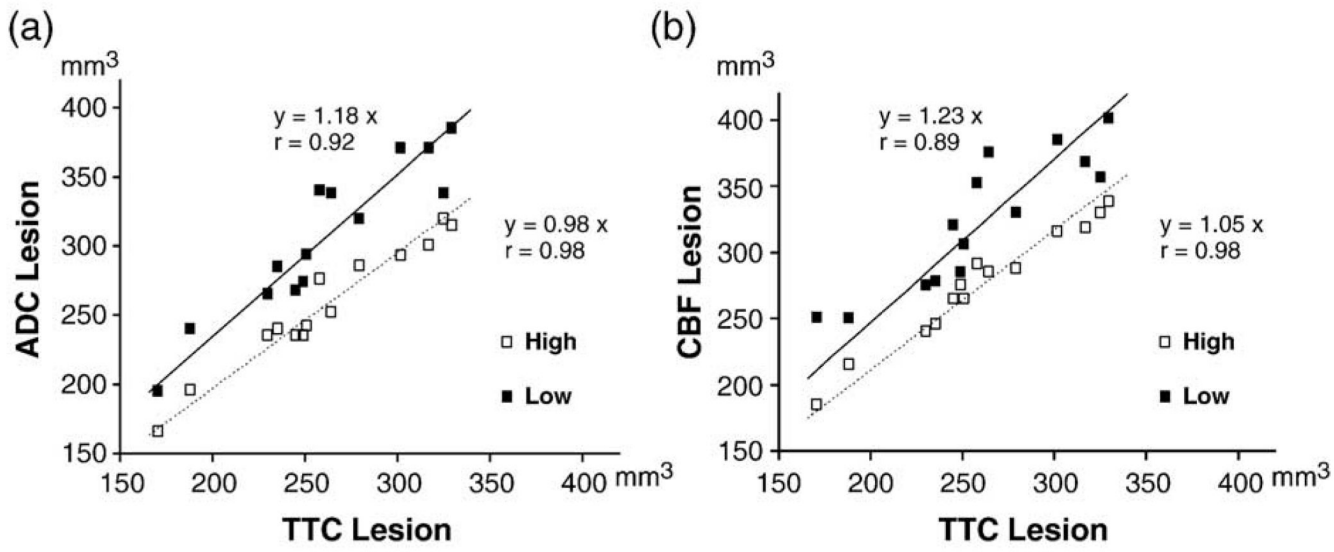

Fig. 3.

Correlation of visually-defined ADC (a) and CBF (b) lesion volumes at 180/200 min after MCAO vs. TTC-defined infarct volumes at 24 h. Closed squares, low-resolution; open squares, high-resolution.

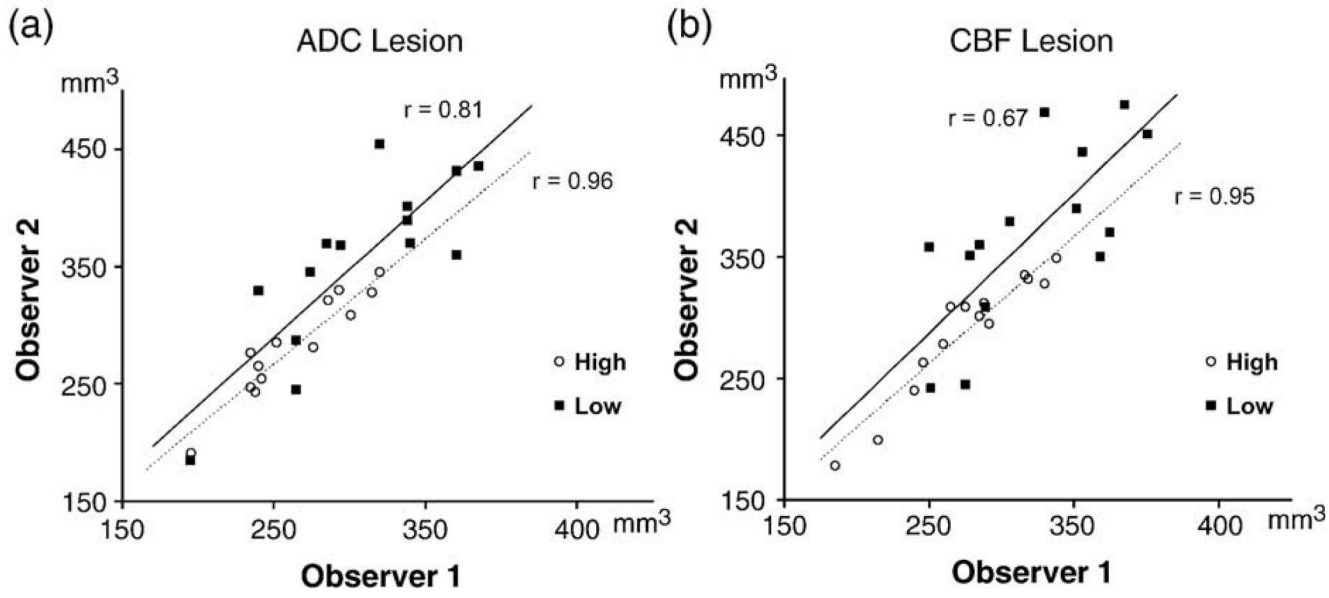

Fig. 4.

Correlation of visually defined lesion volumes between the two observers at 180/200 min after MCAO for ADC (a) and CBF imaging (b). Closed squares, low-resolution; open squares, high-resolution.